iScience

CellPress
OPEN ACCESS

Article

Bacteria associated with the *in hospite* Symbiodiniaceae's phycosphere

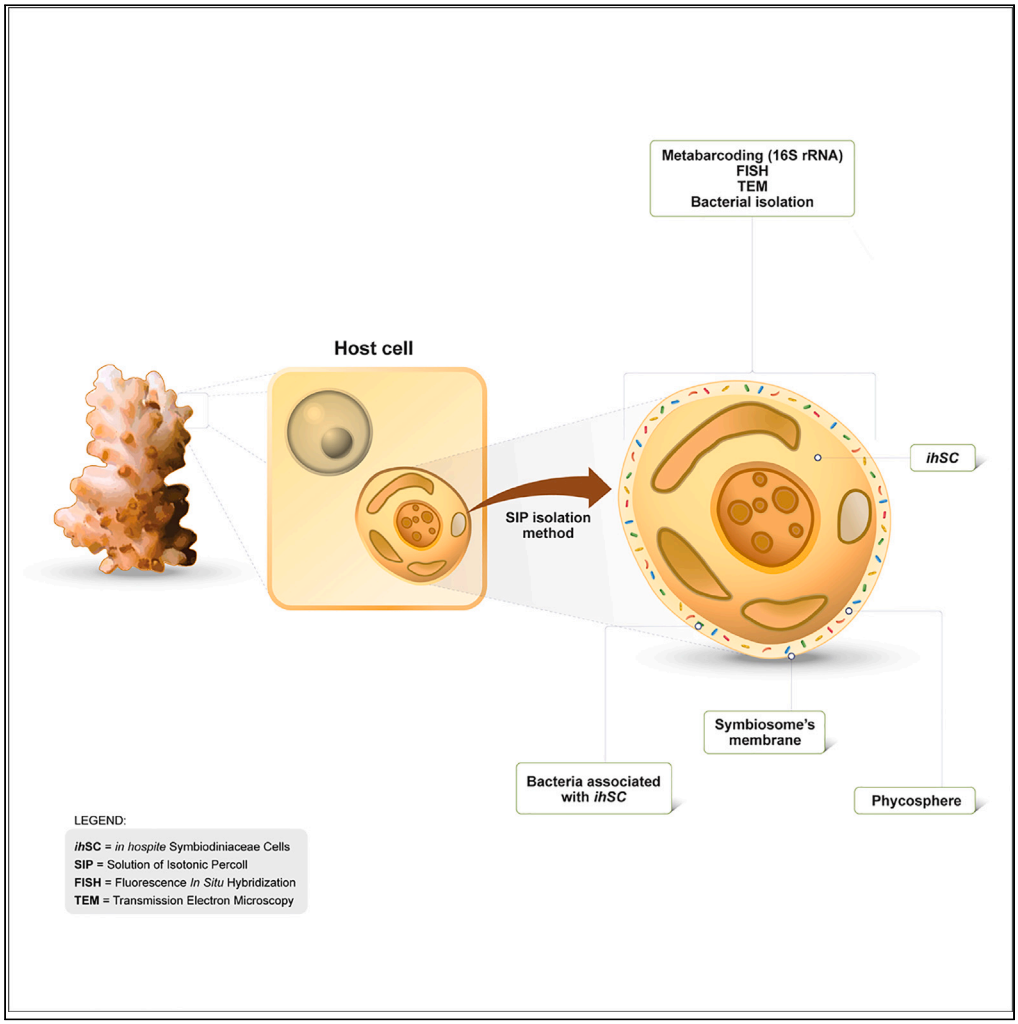

Lilian Jorge Hill, Camila Simões Martins de Aguiar Messias, Caren Leite Spindola Vilela, ..., Flavia Lima do Carmo, Torsten Thomas, Raquel S. Peixoto

raquel.peixoto@kaust.edu.sa

Highlights

New method to study the coral-associated *in hospite* Symbiodiniaceae microbiome

Evidence of extracellular vesicles that can influence *in hospite* phycosphere

Specific ASVs are indicators of samples associated to *in hospite* Symbiodiniaceae

FISH images showed bacteria cells closely associated to *in hospite* Symbiodiniaceae

Hill et al., iScience *27*, 109531
April 19, 2024
https://doi.org/10.1016/j.isci.2024.109531

iScience

CellPress
OPEN ACCESS

Article

Bacteria associated with the *in hospite* Symbiodiniaceae's phycosphere

Lilian Jorge Hill,[1,4] Camila Simões Martins de Aguiar Messias,[1,4] Caren Leite Spindola Vilela,[1] Alessandro N Garritano,[2] Helena Dias Muller Villela,[3] Flavia Lima do Carmo,[1] Torsten Thomas,[2] and Raquel S. Peixoto[3,5,*]

SUMMARY

Symbiotic interactions between Symbiodiniaceae and bacteria are still poorly explored, especially those *in hospite*. Here, we adapted a technique that allows for the enrichment of intact and metabolically active *in hospite* Symbiodiniaceae cells (*ih*SC) and their associated bacteria from the tissue of the model coral *Pocillopora damicornis*, using a discontinuous gradient of solution of isotonic Percoll (SIP). The *ih*SC were concentrated in the 50% SIP fraction, as determined by microscopy. The presence of bacteria associated with *ih*SC was confirmed by fluorescence *in situ* hybridization, while microbiome analysis indicated that bacteria of the families *Halieaceae*, *Flavobacteriaceae*, and *Alcanivoraceae* are significantly associated with *ih*SC. Extracellular vesicles that could be exuding molecules were detected on the symbiosome membranes. Our technique and data contribute to elucidate *ih*SC-bacteria interactions.

INTRODUCTION

The anatomy and ultrastructure of the coral tissue create microenvironments with different microbial assemblages, which have different richness, diversities, activities, and functions within the holobiont.[1,2] For example, the surface mucus layer, coral tissue, and skeleton can harbor distinct microbial communities with different functionalities to the coral host (e.g., microbes that constitute the mucus layer can protect the host against pathogens through antagonistic mechanisms and/or competition).[1,3] Microbial diversity, traits, and symbiotic relationships can be controlled by particular host taxonomies and morphologies (i.e., boulder, branching, plating, solitary).[4–7] At the same time, microbiomes are flexible and also respond to environmental changes.[1–4]

One of the most important symbioses in the coral reef ecosystem occurs between reef-building corals and dinoflagellates from the family Symbiodiniaceae, which has been a key for their widespread distribution and ecological success.[8] The microalgae provide energy for the corals to thrive in oligotrophic environments and, in return, receive shelter and inorganic nutrients.[9] The coral-Symbiodiniaceae relationship also improves coral calcification, thus aiding in the establishment and maintenance of the reef ecosystem.[10] Corals harbor Symbiodiniaceae cells intracellularly in vesicles called symbiosomes,[7] and the region that is directly around the Symbiodiniaceae's cell surface may be influenced by the algae's production of specific metabolites, and is thus referred to as the phycosphere.[11]

Despite the key relationship between corals from shallow reefs (i.e., reefs within the euphotic zone) and Symbiodiniaceae cells, other microbial players, such as bacteria, archaea, fungi, and viruses, are also crucial for the holobiont's development, health, and survival.[12–16] Coral-associated bacteria, for example, drive nutrient cycling, help in the coral's defense against pathogens, degrade toxic compounds, and enhance the holobiont's tolerance to different stressors.[17–21] Recent studies demonstrated that beneficial microorganisms for corals (BMC) and other microbial-based therapies can be actively used as "customized medicine" to support conservation and restoration/rehabilitation efforts[16,18,21–29] and that associations between a coral and its microbiome, and also between *in hospite* Symbiodiniaceae (*ih*SC) and other microorganisms, could be good targets for these microbial-based therapies.[16,18,30] The presence of bacteria inside and outside Symbiodiniaceae and the presence of specific core bacteria shared between different species of cultured free-living Symbiodiniaceae have already been shown.[31,32] However, despite the potential importance of Symbiodiniaceae-associated microorganisms for coral nutrition (e.g., contributing to Symbiodiniaceae growth and health, and the consequent translocation of organic compounds to the host),[15,33] the relationship between the *ih*SC and their associated bacteria is still poorly understood.

Symbiodiniaceae extraction (including some intact symbiosomes), enrichment, and purification have never been successfully performed on scleractinian corals or used to explore the *ih*SC-associated microbiome. Here, we adapt a protocol previously used to purify the

[1]Laboratory of Molecular Microbial Ecology, Institute of Microbiology Paulo de Góes, Federal University of Rio de Janeiro, Rio de Janeiro 21941-901, Brazil
[2]Centre for Marine Science and Innovation, School of Biological, Earth and Environmental Sciences, The University of New South Wales, Sydney, NSW, Australia
[3]Red Sea Research Center, Biological and Environmental Science and Engineering Division, King Abdullah University of Science and Technology, Thuwal 23955, Kingdom of Saudi Arabia
[4]These authors contributed equally
[5]Lead contact
*Correspondence: raquel.peixoto@kaust.edu.sa
https://doi.org/10.1016/j.isci.2024.109531

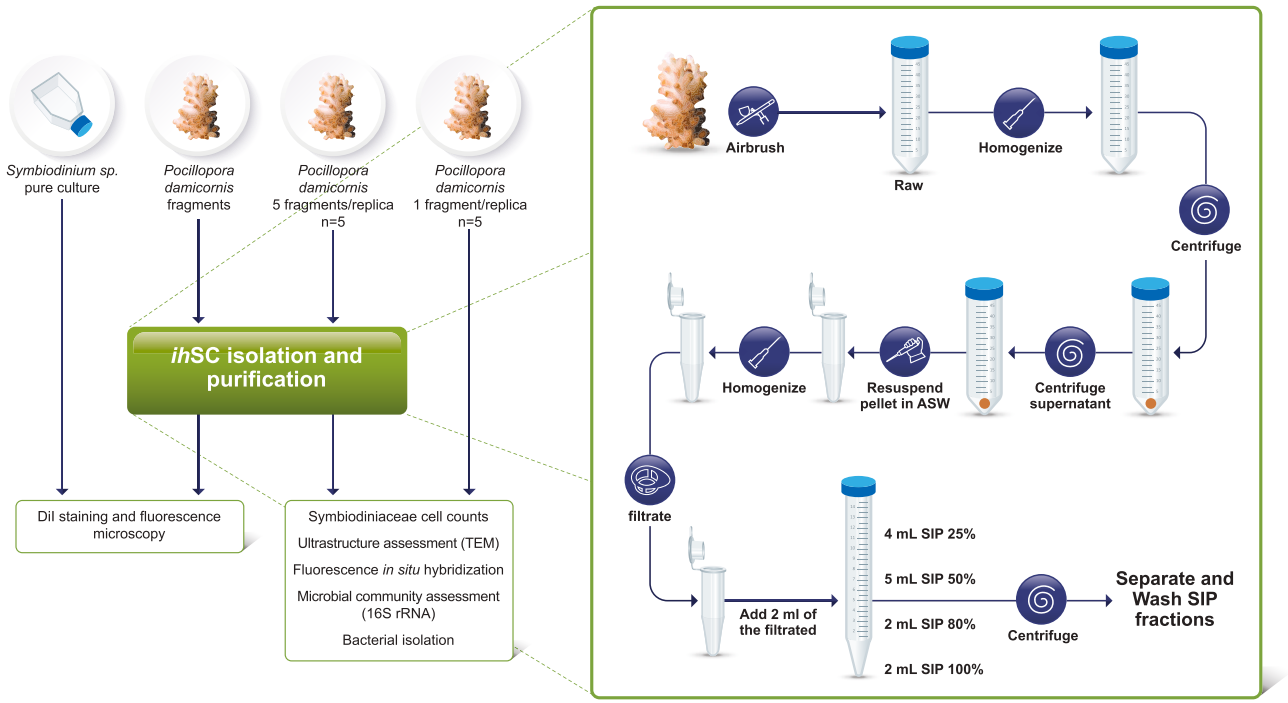

Figure 1. General stepwise of the protocol for cellular fractionation and purification of Symbiodiniaceae-associated bacteria

The integrity of Symbiodiniaceae cells was first examined, using fragments of *P. damicornis* and *Symbiodinium* sp. pure culture as a positive control. The cellular fractionation and separation protocol validation was then performed using a total of 30 *P damicornis* fragments (i.e., one sample composed of seven fragments, for the obtention of enough biomass, was used for each experiment, which was repeated five times—n = 5) and five coral fragments for the raw tissue samples (i.e., n = 5) as a positive control.

symbiosomes (i.e., vesicles containing Symbiodiniaceae) from zoanthids and Aiptasia[34,35] and apply it to coral tissue, aiming to recover the Symbiodiniaceae cells and their associated microbiome. The protocol is based on the mechanical separation of tissue, followed by successive centrifugations, including a solution of isotonic Percoll (SIP) discontinuous gradient (i.e., 0%, 25%, 50%, 80%, and 100% SIP fractions), to separate different density fractions. We then use a variety of microscopy and molecular tools to validate the method and access the microbiome associated with *ih*SC. We also explore specific bacteria that are significantly associated with *ih*SC and propose that this methodology, developed using the model coral *Pocillopora damicornis*, can be expanded to other coral species.

RESULTS

The method proposed in the present study is based on the fractionation of coral tissue and separation of the structures using both the discontinuous SIP gradient and raw coral tissue samples (i.e., coral tissue before being subjected to the SIP gradient). Our protocol uses different centrifugation regimes and includes microscopy to evaluate the separation and integrity of Symbiodiniaceae cells. Moreover, we used culture dependent and independent methods to access the microbiome associated with *ih*SC, as well as fluorescence *in situ* hybridization (FISH) to localize bacteria cells. An overview of the method is illustrated in Figure 1.

Recovery of intact and viable *in hospite* Symbiodiniaceae cells

Analysis of ITS2 sequences of the raw coral sample and all SIP fractions showed a dominance of *Cladocopium* sp., followed by *Symbiodinium* sp. as the main photosymbionts in *P. damicornis* (Figure S2). *Breviolum* sp. and *Durusdinium* sp. were also detected, although they were less abundant (<1% relative abundance).

Each fraction obtained after SIP processing was counted in a Neubauer chamber to determine the fraction with the highest number of Symbiodiniaceae cells. The 50% SIP fraction had the highest Symbiodiniaceae cell count (9.6×10^5 cells/mL; Kruskal-Wallis $p = 0.008$), although this was not significantly different compared to the 0% and 25% SIP fractions (Figures 2A and S3; Dunn's test $p > 0.6$), but different from the other fractions (i.e., 80% and 100% SIP fractions; Dunn's test $p < 0.008$). Consequently, further microscopy analysis (see in the following section) was performed using the fraction with one of the highest Symbiodiniaceae counts (50% SIP fraction) and the raw samples.

The integrity of Symbiodiniaceae cells and, eventually, the presence of symbiosomes, from the 50% SIP fraction were assessed to evaluate if the separation and purification process would damage the algal cells. Fluorescent images using DiI stain showed that Symbiodiniaceae membranes remained intact after the purification process (Figure 2B). Samples taken from the 50% SIP fraction had similar DiI fluorescence

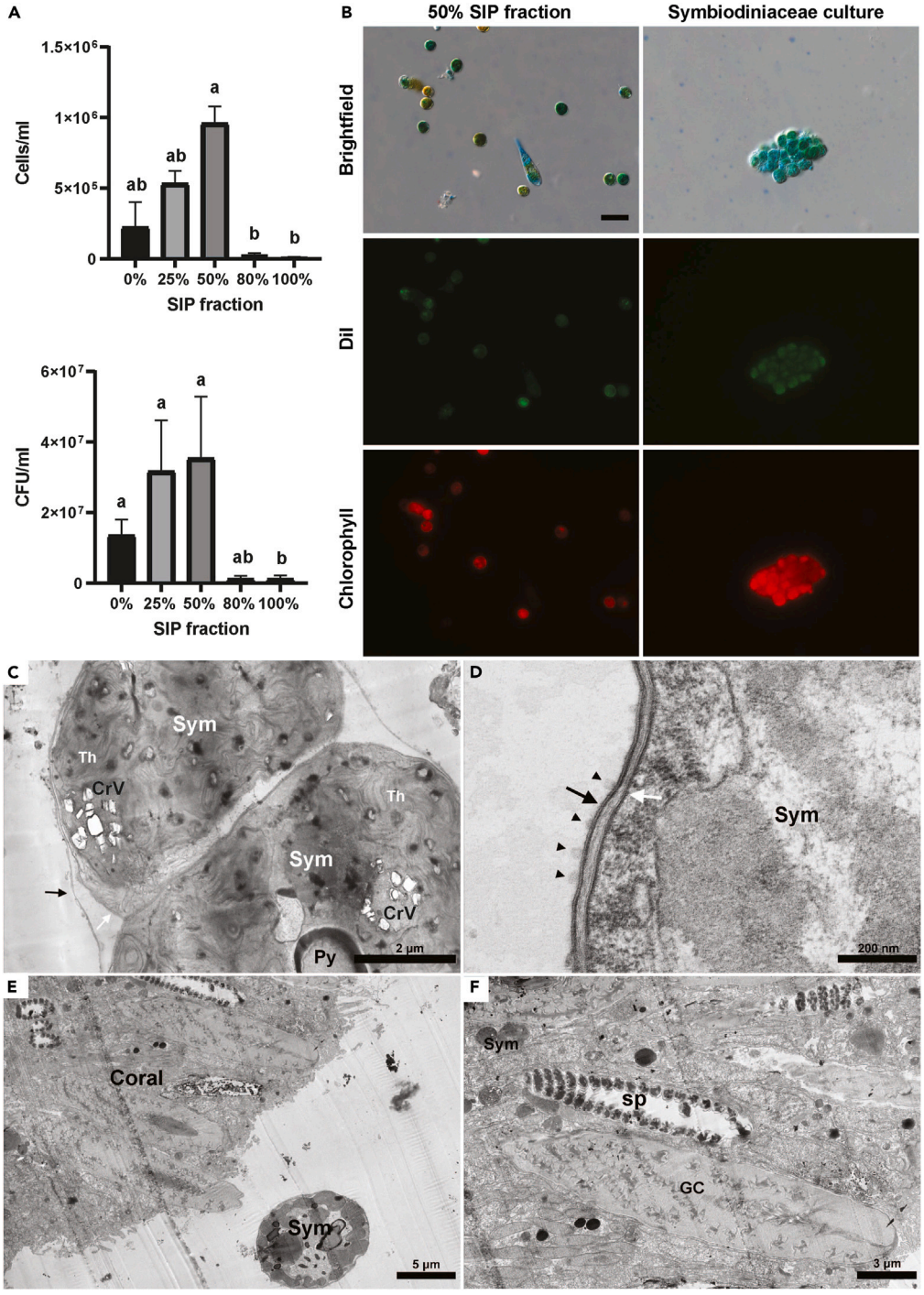

Figure 2. The 50% SIP fraction showed the highest Symbiodiniaceae counts and preserved symbiosome membranes

(A) Symbiodiniaceae cell counts and CFU counts on each fraction.

(B) Fluorescent micrographs of Symbiodiniaceae cells from the 50% SIP fraction and Symbiodiniaceae cultures (CCMR0100—*Symbiodinium* sp.) stained with DiI to verify membrane integrity. The speckly background is an artifact of the microscope objectives. The DiI stain may look blueish to the naked eye (i.e., not excited by laser) when accumulated in the cell membranes. DiI is displayed in green and chlorophyll is displayed in red. Bars = 20 µm.

(C–F) Transmission electron micrographs of the 50% fraction (C and D) and raw coral tissue (E and F) samples from *Pocillopora damicornis*. (E) Is a higher magnification of figure (F) that shows top slices of ihSC, identified due to unique characteristics (e.g., uric acid crystals and chloroplasts). Sym, Symbiodiniaceae cells; Th, thylakoid membranes; CrV, uric acid crystals vesicles; black arrowheads, putative extracellular vesicle; black arrows, outer symbiosome's membrane; white arrows, inner Symbiodiniaceae cell membrane; coral, coral tissue; sp, spirocysts; GC, gland cells.

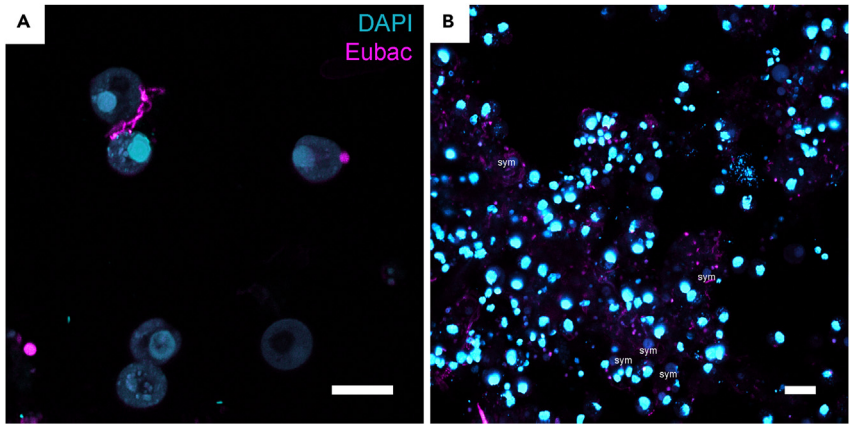

Figure 3. Fluorescence *in situ* hybridization images using the Eub-388 probe (magenta) and DAPI staining (blue)

(A) Bacterial cells associated with Symbiodiniaceae cells in the 50% SIP fraction.

(B) Bacterial cells associated with coral tissues and Symbiodiniaceae within coral tissue (*sym*) from raw samples. Symbiodiniaceae nuclear labeling is fainter than coral nuclei in tissue samples. Bars = 10 μm. Images with NonEub antisense probe for negative FISH control can be found in supplementary material (Figure S5). An example of an unprocessed confocal laser scanning micrograph is available in Figure S6.

to those taken from free-living Symbiodiniaceae cultures. Furthermore, transmission electron microscopy (TEM) images of the cells from the 50% SIP fraction also showed the presence of intact inner and outer symbiosome membranes, as well as what appeared to be extracellular vesicles (EVs) attached to the outer symbiosome membrane (Figures 2C and 2D). Images of raw samples showed coral tissue with few Symbiodiniaceae cells *in hospite* and *ex hospite* adjacent to the coral tissue (Figures 2E and 2F). Additionally, Symbiodiniaceae cells showed a relatively well-preserved ultrastructure even after the centrifugation, typical ultrastructure with reticulated chloroplasts with organized thylakoids and intact membranes, vacuoles, and nuclei with condensed chromosomes, again indicating that the cellular fractionating did not affect the integrity of the cells.

Additionally, lower magnification TEM images (Figure S4) confirmed the dominance of Symbiodiniaceae cells in the 50% SIP fraction. Only a small amount of cell debris was observed in this fraction, probably membrane fragments derived from host cells, while the raw samples contained whole coral tissue and different types of loose coral cells.

Bacteria associated with *in hospite* Symbiodiniaceae cells

FISH images using a general bacterial probe (Figure 3) revealed bacterial cells closely associated with *ih*SC cells in the 50% SIP fraction (Figure 3A; Video S1). Additionally, images taken straight after the airbrush step (i.e., raw samples) also showed several bacterial cells and aggregates around Symbiodiniaceae cells within the coral tissue (Figure 3B; Video S2). Symbiodiniaceae cells within coral tissue in raw samples were identified by typical morphology and through chlorophyll autofluorescence (refer to Figure S6 to see an unprocessed image of the raw sample with the chlorophyll channel).

Viable bacterial cells were cultured from all fractions. Samples from 100% SIP fraction showed the lowest colony forming unit (CFU) counts (Figure 2I; Kruskal-Wallis test $p = 0.0129$; Dunn's multiple comparisons test $p = 0.0425$). There were no statistical differences between the other SIP fractions (Figure 2I; Dunn's test $p > 0.4$). Negative control plates showed no bacterial growth.

For a comprehensive comparison of the *ih*SC-associated microbiome, we performed 16S rRNA gene amplicon sequencing on samples from the different SIP fractions as well as raw samples. *Pseudomonadota* was the dominant phylum in all SIP fractions and raw samples, specifically represented by the families *Alteromonadaceae* and *Vibrionaceae* (Figure 4A). Raw samples had higher microbial alpha diversity indexes in comparison to the SIP fractions—i.e., Chao1 index (Kruskal-Wallis and Wilcoxon, $p < 0.03$) and Shannon diversity index (Kruskal-Wallis and Wilcoxon, $p < 0.02$) (Figure 4B). Higher Chao1 indexes were also observed in samples from the upper SIP fractions (i.e., 0%, 25%, and 50%) compared to samples from the lower SIP fractions (i.e., 80% and 100%) (Kruskal-Wallis and Wilcoxon, $p < 0.05$) (see Table S1 for further detail).

A separation based on the beta diversity of microbial community structure was clearly observed for the raw samples and the Percoll fractions (Figure 4C). We found a significant difference in the microbial community structure (PERMANOVA based on Bray-Curtis dissimilarity, $p = 0.001$; Table S2) and composition (PERMANOVA based on Sorensen's dissimilarity, $p = 0.001$; Table S3) between SIP fractions. Pairwise comparisons revealed differences in microbial community structure between the raw samples and all SIP fractions ($p < 0.02$) and between 50% vs. 80% SIP fractions ($p = 0.043$) and 50% vs. 100% ($p = 0.039$). Regarding microbial community composition, pairwise comparisons also showed differences between raw samples and all SIP fractions and between the upper SIP fractions versus the lower SIP fractions (i.e., 0%, 25%, and 50% vs. 80% and 100%; $p < 0.03$) (see Table S3 for further detail).

Although permutational multivariate analysis of dispersion (PERMDISP) showed no significant differences in the dispersions of the microbial community structures of the different SIP fractions and raw samples (PERMDISP based on Bray-Curtis' dissimilarity, $p = 0.8762$; Table S4; Figure S5A), the dispersions of the microbial community compositions between raw samples significantly differed to those of all SIP fractions

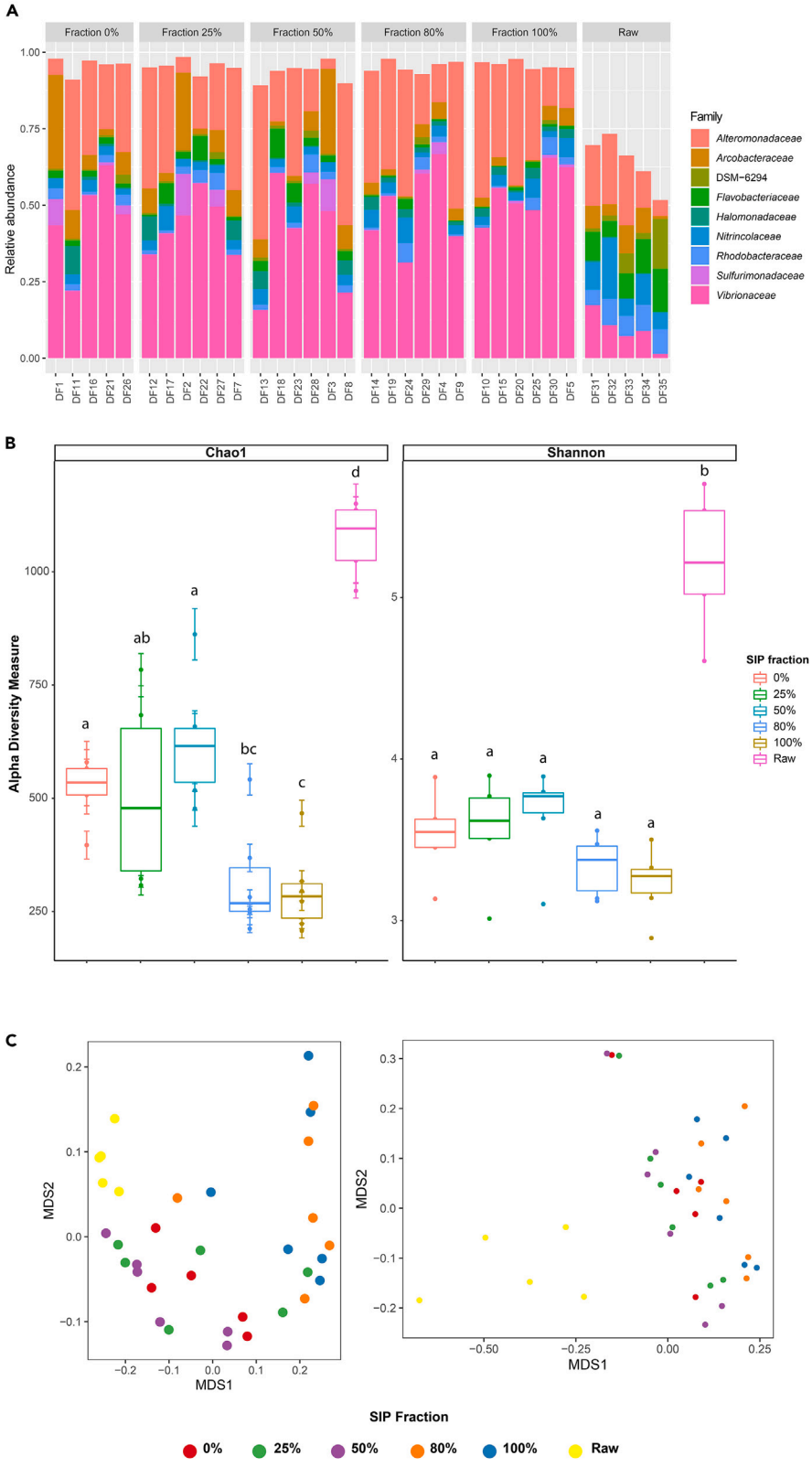
A
Fraction 0%
Fraction 25%
Fraction 50%
Fraction 80%
Fraction 100%
Raw
Relative abundance
Family
Alteromonadaceae
Arcobacteraceae
DSM−6294
Flavobacteriaceae
Halomonadaceae
Nitrincolaceae
Rhodobacteraceae
Sulfurimonadaceae
Vibrionaceae
B
Chao1
Shannon
Alpha Diversity Measure
SIP fraction
0%
25%
50%
80%
100%
Raw
C
MDS1
MDS2
SIP Fraction
0%
25%
50%
80%
100%
Raw

Figure 4. Microbial community associated with *in hospite* Symbiodiniaceae from *Pocillopora damicornis*

(A) Taxonomic profile and relative abundance of bacterial families obtained from SIP fractions and raw samples. X axis represent each sample.

(B) Alpha-diversity of each SIP fraction (different letters on top of bars represent statistical difference; Kruskal-Wallis and Willcoxon post-hoc tests, $p < 0.05$—see Table S1 for more information).

(C) Beta-diversity represented in an nMDS based on Sorensen's similarity (left; stress value: 0.03485008), and on Bray-Curtis dissimilarity (right; stress value: 0.1188355) of each SIP fraction.

(PERMDISP based on Sorensen's dissimilarity, $p = 0.001214$; Tukey honestly significant difference - HSD- , $p < 0.049$; Table S5; Figure S5B). However, no significant differences in dispersions between SIP fractions were observed (Tukey HSD, $p > 0.6$; Table S5).

To investigate the enrichment or exclusivity of some microbial groups in each fraction or raw samples, we performed an indicator species analysis using a significant cut-off level (alpha) of 0.02. This analysis allowed us to assess the statistical strength (p value) and significance (stat value) between the ASVs (amplicon sequence variant) occurrence/abundance and the fractions and to select significant ASVs associated with one or more fractions by ordering the ASVs through values of specificity (a value) and fidelity (b value). The results indicated that raw samples (which can also include superficial parts of the coral skeleton and its associated microbiome) had characteristic ASVs that differentiate their microbial communities from those of the SIP fractions. Interestingly, this analysis also showed that three ASVs were significantly associated only with samples from the 50% SIP fraction (Figure 5). These ASVs were assigned to the taxa *Confluentibacter flavum* (family *Flavobacteriaceae*; ASV1284; stat = 0.74, p = 0.012, a = 0.8333, b = 0.6667), *Halioglobus* sp. (family *Halieaceae*; ASV2117; stat = 0.77, p = 0.007, a = 0.8929, b = 0.6667), and an *Alcanivorax* sp. (family *Alcanivoraceae*, ASV1035, stat = 0.8, p = 0.019, a = 0.6406, b = 1.000). Together, these three ASVs comprised 0.027% of the total read abundance in the 50% SIP fraction. Importantly, we only detected ASVs significantly associated with either the 50% fraction or raw samples, but not with the other fractions (see Table S6). Moreover, only the upper SIP fractions (i.e., 0%, 25%, and 50%) shared ASVs with the raw samples (i.e., 0% vs. raw; 25% vs. raw; 50% vs. raw), while the lower SIP fractions (i.e., 80% and 100%) only shared ASV's with each other (i.e., 80% vs. 100%) but not with the upper SIP fractions or the raw samples. All other shared ASVs were found in three or more groups of samples.

Finally, a total of 37 bacterial isolates, representing randomly selected different morphotypes, were obtained across the SIP gradient samples. We compared sequences of isolates to sequences of ASVs retrieved from the 16S rRNA gene amplicon sequencing data. Isolate sequences were matched with 100% identity cut-off (but allowing for one gap in homopolymer regions) ASV sequences. Out of these 37 isolates, 27 matched to seven different ASVs with the following taxonomies: eight to *Vibrio hyugaensis*, nine to *Vibrio fortis*, three to *Vibrio alfacsensis*, four to *Pseudoalteromonas* sp., one to *Alteromonas abrolhosensis*, one to *Cobetia marina*, and one to *Pseudoalteromonas luteoviolacea* (Table S7). Together, these ASVs had an average relative abundance that ranged from ~5% (in the raw samples) to ~26% (in the 100% SIP fraction) (Figure S8).

DISCUSSION

This study is the first to present a feasible, affordable, and cohesive method to recover intact coral-associated Symbiodiniaceae cells *in hospite* to study its associated bacterial diversity. A recent study[36] used repeated centrifugations of the airbrushed tissue of *Acropora aspera* to isolate *ih*SC, although there is no evidence that the authors were able to recover intact symbiosomes or Symbiodiniaceae cells (i.e., no microscopy images). The method developed in our study is based on the rupture of the coral tissue and separation of the subcellular compartments through a discontinuous Percoll gradient.[35,37] Here, TEM images confirmed the separation of intact Symbiodiniaceae cells from the coral tissue while still maintaining the symbiosome membrane. The preservation of the symbiosome membrane is ideal for accessing bacteria that are closely associated with these photosymbionts, and confocal laser scanning microscope images using a general bacterial FISH probe confirmed the presence of bacteria adjacent to the Symbiodiniaceae cells from the 50% SIP fraction.

While we observed a higher concentration of Symbiodiniaceae cells in the 50% SIP fraction, Peng et al. (2010)[35] found the highest concentration of photosymbionts in 80% and 100% SIP fractions using a similar method to investigate protein components of the symbiosome membranes of the sea anemone *Exaiptasia* spp. Since this method is based on a differential separation by density, the volume and mass of the host and its photosymbionts cells directly influence the distribution along the discontinuous Percoll gradient. This indicates that the Symbiodiniaceae-enriched SIP fraction may vary depending on the host (i.e., Aiptasia vs. coral) and potentially even different coral species. Therefore, future analysis of the fraction for other coral species should be guided by microscopy and Symbiodiniaceae cell counts.

Differential bacterial counts were detected among the fractions of the discontinuous gradient of SIP, which may be related to the different cellular and tissue compartments of the host that were collected by airbrushing (e.g., coral mucus, coral tissue, Symbiodiniaceae phycosphere).[1,2,38] The genera found in our isolates (i.e., *Vibrio*, *Alteromonas*, *Pseudoalteromonas*, and *Cobetia*) are widely reported to be associated with different coral species.[23,39–41]

There are records that *Pseudoalteromonas luteoviolacea*, one of the bacterial isolates obtained from the 50% SIP fraction, produces molecules that inhibit the growth of pathogens, such as *V. harveyi* and *V. corallilyticus*.[42,43] By potentially occupying the *in hospite* Symbiodiniaceae phycosphere, *P. luteoviolacea* may contribute to the biological control of pathogens potentially associated with the phycosphere. We suggest that this species and its functional traits should be further investigated for potential BMC traits.

Marinobacter, *Labrenzia*, *Muricauda*, and an unidentified species of *Chromaticeae* have been previously identified as members of the core microbiome associated with cultured Symbiodiniaceae,[31,32] while *Hyphomicrobium*, *Methylobacterium*, and *Sphyngomonas* were identified as the most abundant genera to occur intracellularly in cultured Symbiodiniaceae from 11 different strains.[32] Although we have identified in our samples ASVs from the same genera as previously detected intracellularly, as well as ASVs from the genus *Marinobacter*, we did not detect ASVs from the genera *Labrenzia* and *Muricauda*.

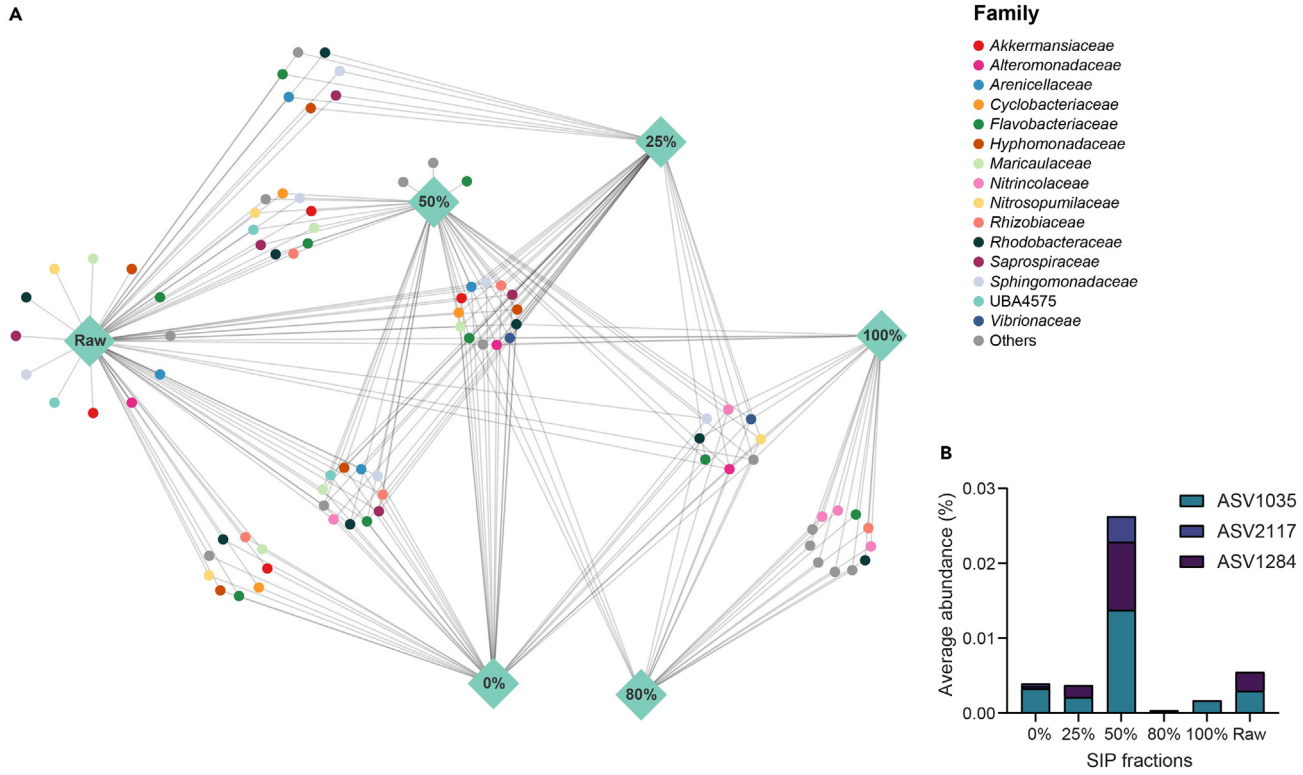

Figure 5. Indicator species analysis shownig significant ASVs associated with one or more SIP fractions

(A and B) Network plot (A) showing ASVs (circles) that differentiate and best characterize each fraction (diamonds) and ASVs that are shared between fractions. ASVs are colored according to family. The relative abundances of the three ASVs that characterize the 50% SIP fraction are shown in (B).

The 50% SIP fraction, which had the highest concentration of *ih*SC was also the only fraction to present specific and significantly associated ASVs, belonging to the taxa *Halioglobus* sp. (*Halieaceae*), *Confluentibacter flavum* (*Flavobacteriaceae*), and *Alcanivorax* sp. (*Alcanivoraceae*). These groups can perform essential roles that might support *ih*SC and its symbiosis with corals. For instance, *Halieaceae* is a relatively recently discovered family,[44] and the *Halioglobus* genus was reported to be involved in denitrification processes.[44] Although Symbiodiniaceae cells are crucial in absorbing nitrogen in the coral holobiont,[45] excess nitrogen must be eliminated to help maintain the N:P ratio and, therefore, avoid bleaching susceptibility.[46] This process can be done by denitrifying microorganisms.[47] Members of the *Alcanivorax* genus are some of the most abundant groups found in coral adults[48] and recruits[49] and, this genus is known to degrade hydrocarbon derivatives.[50,51] Furthermore, the *Alcanivorax* genus has been found in close association with the microalgae *Nannochloropsis oculata* and *Pavlova lutheri*.[52] These microbial groups could represent part of the microbiome associated with *ih*SC in *P. damicornis* and should be further investigated in terms of their potential role as coral probiotics.[16,18,53]

Additionally, we found that the overall microbial communities differ between SIP fractions, specifically the 50% SIP fraction in comparison with the denser fractions (i.e., 80% and 100%). The SIP fractions in which the highest numbers of *ih*SCs were found (i.e., 0%, 25%, and 50%) also showed a higher microbial richness (Kruskal-Walis and Wilcoxon rank; $p < 0.05$), which indicates the potential influence that Symbiodiniaceae cells may have on the microbial community within the coral holobiont.[38] This phenomenon is similar to the microbiome modulation in plant rhizospheres and its correlation with plant health.[54] This hypothesis was also raised by Gardner et al.,[36] as their centrifuged samples also presented a distinct microbiome, when compared to the raw *A. aspera* host.

Free-living Symbiodiniaceae can influence their surrounding microbiome by exudating specific metabolites that create the phycosphere,[11,15,38,55–57] and here we provide a tool to recover intact Symbiodiniaceae cells and their associated microbiomes from coral tissues. In addition, recent data indicate that EVs may play an important role in creating the phycosphere[58] and for mediating endosymbiosis.[59] Our TEM images revealed structures on the symbiosome membranes (see Figure 4B) that could be EVs, which could be involved in the translocation of photosynthates. An alternative hypothesis is that Symbiodiniaceae cells inside coral tissue may exude molecules inside these EVs, which could help recruit specific microbial cells to their *in hospite* phycosphere,[11,15,38,55–57] similar to what is observed in plant rhizospheres.[60,61] Further studies are necessary to explore these EVs and their role in coral-*ih*SC symbiosis.

Combined, our results indicate that the method we adapted and validated can be used to differentiate the microbiome associated with different structures of the coral holobiont. In addition, this method allows us to obtain and explore the biotechnological potential of bacterial metabolites in association with different coral tissue and cellular compartments.

Limitations of the study

Our study lays the ground for important advances toward the investigation of how bacteria associated with *ih*SC may be playing roles in the coral holobiont's health. However, the results presented here are limited to the model studied (i.e., *Pocillopora damicornis*) and, therefore, it is important to test this methodology in other coral (or even other Cnidarian) species. Our methodology could facilitate acquiring *ih*SC (eventually including their symbiosome) and their closely associated microorganisms, however, the washing steps necessary for this method may remove some of the loosely associated microbes. Nonetheless, this methodology represents an important, affordable, and feasible way to further investigate *ih*SC-associated microorganisms.

STAR★METHODS

Detailed methods are provided in the online version of this paper and include the following:

- KEY RESOURCES TABLE
- RESOURCE AVAILABILITY
  - Lead contact
  - Materials availability
  - Data and code availability
- EXPERIMENTAL MODEL AND STUDY PARTICIPANT DETAILS
- METHOD DETAILS
  - Cellular fractionation and in hospite symbiodiniaceae purification
  - Cellular integrity assessment of symbiodiniaceae fraction
  - Analysis of *in hospite* symbiodiniaceae-associated bacteria
- QUANTIFICATION AND STATISTICAL ANALYSIS

SUPPLEMENTAL INFORMATION

Supplemental information can be found online at https://doi.org/10.1016/j.isci.2024.109531.

ACKNOWLEDGMENTS

The authors would like to thank Instituto de Pesquisas Jardim Botânico do Rio de Janeiro (JBRJ) and Instituto Museu Aquário Marinho do Rio de Janeiro-AquaRio (IMAM/AquaRio)—Rio de Janeiro Marine Aquarium Research Center, Rio de Janeiro, Brazil. This study was carried out in association with the R&D project registered as ANP 21005-4 (UFRJ/Shell Brasil/ANP), sponsored by Shell Brasil under the ANP R&D levy as "Compromisso de Investimentos com Pesquisa e Desenvolvimento".

AUTHOR CONTRIBUTIONS

Conceptualization: L.J.H., C.S.M.A.M., C.L.S.V., H.D.M.V., and R.S.P.; methodology: L.J.H., C.S.M.A.M., C.L.S.V., H.D.M.V., and R.S.P.; investigation: L.J.H., C.S.M.A.M., and C.L.S.V.; formal analysis: L.J.H., C.S.M.A.M., and A.N.G.; resources: F.L.C., T.T., and R.S.P.; data curation: L.J.H., and A.N.G.; writing – original draft: L.J.H. and C.S.M.A.M. ; writing – reviewing & editing: L.J.H., C.S.M.A.M., C.L.S.V., H.D.M.V., A.N.G., F.L.C., T.T., and R.S.P; visualization: L.J.H. and A.N.G.; supervision: F.L.C., T.T., and R.S.P.; project administration: F.L.C., T.T., and R.S.P.; funding acquisition: T.T. and R.S.P.

DECLARATION OF INTERESTS

The authors declare no competing interests.

Received: May 16, 2023
Revised: December 23, 2023
Accepted: March 16, 2024
Published: March 19, 2024

REFERENCES

1. Sweet, M.J., Croquer, A., and Bythell, J.C. (2011). Bacterial assemblages differ between compartments within the coral holobiont. Coral Reefs *30*, 39–52. https://doi.org/10.1007/s00338-010-0695-1.
2. Hughes, D.J., Raina, J.-B., Nielsen, D.A., Suggett, D.J., and Kühl, M. (2022). Disentangling compartment functions in sessile marine invertebrates. Trends Ecol. Evol. *37*, 740–748. https://doi.org/10.1016/j.tree.2022.04.008.
3. Glasl, B., Herndl, G.J., and Frade, P.R. (2016). The microbiome of coral surface mucus has a key role in mediating holobiont health and survival upon disturbance. ISME J. *10*, 2280–2292. https://doi.org/10.1038/ismej.2016.9.
4. Ziegler, M., Grupstra, C.G.B., Barreto, M.M., Eaton, M., BaOmar, J., Zubier, K., Al-Sofyani, A., Turki, A.J., Ormond, R., and Voolstra, C.R. (2019). Coral bacterial community structure responds to environmental change in a host-specific manner. Nat. Commun. *10*, 3092. https://doi.org/10.1038/s41467-019-10969-5.
5. Morrow, K.M., Pankey, M.S., and Lesser, M.P. (2022). Community structure of coral microbiomes is dependent on host

morphology. Microbiome *10*, 113. https://doi.org/10.1186/s40168-022-01308-w.
6. Leite, D.C.A., Salles, J.F., Calderon, E.N., Castro, C.B., Bianchini, A., Marques, J.A., Van Elsas, J.D., and Peixoto, R.S. (2018). Coral Bacterial-Core Abundance and Network Complexity as Proxies for Anthropogenic Pollution. Front. Microbiol. *9*, 833. https://doi.org/10.3389/fmicb.2018.00833.
7. Leite, D.C.A., Salles, J.F., Calderon, E.N., Van Elsas, J.D., and Peixoto, R.S. (2018). Specific plasmid patterns and high rates of bacterial co-occurrence within the coral holobiont. Ecol. Evol. *8*, 1818–1832. https://doi.org/10.1002/ece3.3717.
8. Muller-Parker, G., D'Elia, C.F., and Cook, C.B. (2015). Interactions Between Corals and Their Symbiotic Algae. In Coral Reefs in the Anthropocene, C. Birkeland, ed. (Springer Netherlands), pp. 99–116. https://doi.org/10.1007/978-94-017-7249-5_5.
9. Cunning, R., Muller, E.B., Gates, R.D., and Nisbet, R.M. (2017). A dynamic bioenergetic model for coral- Symbiodinium symbioses and coral bleaching as an alternate stable state. J. Theor. Biol. *431*, 49–62. https://doi.org/10.1016/j.jtbi.2017.08.003.
10. Inoue, M., Nakamura, T., Tanaka, Y., Suzuki, A., Yokoyama, Y., Kawahata, H., Sakai, K., and Gussone, N. (2018). A simple role of coral-algal symbiosis in coral calcification based on multiple geochemical tracers. Geochem. Cosmochim. Acta *235*, 76–88. https://doi.org/10.1016/j.gca.2018.05.016.
11. Bell, W., and Mitchell, R. (1972). CHEMOTACTIC AND GROWTH RESPONSES OF MARINE BACTERIA TO ALGAL EXTRACELLULAR PRODUCTS. Biol. Bull. *143*, 265–277. https://doi.org/10.2307/1540052.
12. Rosenberg, E., Koren, O., Reshef, L., Efrony, R., and Zilber-Rosenberg, I. (2007). The role of microorganisms in coral health, disease and evolution. Nat. Rev. Microbiol. *5*, 355–362. https://doi.org/10.1038/nrmicro1635.
13. Raina, J.-B., Tapiolas, D., Willis, B.L., and Bourne, D.G. (2009). Coral-Associated Bacteria and Their Role in the Biogeochemical Cycling of Sulfur. Appl. Environ. Microbiol. *75*, 3492–3501. https://doi.org/10.1128/AEM.02567-08.
14. Amend, A.S., Barshis, D.J., and Oliver, T.A. (2012). Coral-associated marine fungi form novel lineages and heterogeneous assemblages. ISME J. *6*, 1291–1301. https://doi.org/10.1038/ismej.2011.193.
15. Matthews, J.L., Raina, J.B., Kahlke, T., Seymour, J.R., van Oppen, M.J.H., and Suggett, D.J. (2020). Symbiodiniaceae-bacteria interactions: rethinking metabolite exchange in reef-building corals as multi-partner metabolic networks. Environ. Microbiol. *22*, 1675–1687. https://doi.org/10.1111/1462-2920.14918.
16. Peixoto, R.S., Sweet, M., Villela, H.D.M., Cardoso, P., Thomas, T., Voolstra, C.R., Høj, L., and Bourne, D.G. (2021). Coral Probiotics: Premise, Promise, Prospects. Annu. Rev. Anim. Biosci. *9*, 265–288. https://doi.org/10.1146/annurev-animal-090120-115444.
17. Ritchie, K. (2006). Regulation of microbial populations by coral surface mucus and mucus-associated bacteria. Mar. Ecol. Prog. Ser. *322*, 1–14. https://doi.org/10.3354/meps322001.
18. Peixoto, R.S., Rosado, P.M., Leite, D.C.D.A., Rosado, A.S., and Bourne, D.G. (2017). Beneficial Microorganisms for Corals (BMC): Proposed Mechanisms for Coral Health and Resilience. Front. Microbiol. *8*, 341. https://doi.org/10.3389/fmicb.2017.00341.
19. Ziegler, M., Seneca, F.O., Yum, L.K., Palumbi, S.R., and Voolstra, C.R. (2017). Bacterial community dynamics are linked to patterns of coral heat tolerance. Nat. Commun. *8*, 14213. https://doi.org/10.1038/ncomms14213.
20. Robbins, S.J., Singleton, C.M., Chan, C.X., Messer, L.F., Geers, A.U., Ying, H., Baker, A., Bell, S.C., Morrow, K.M., Ragan, M.A., et al. (2019). A genomic view of the reef-building coral Porites lutea and its microbial symbionts. Nat. Microbiol. *4*, 2090–2100. https://doi.org/10.1038/s41564-019-0532-4.
21. Santoro, E.P., Borges, R.M., Espinoza, J.L., Freire, M., Messias, C.S.M.A., Villela, H.D.M., Pereira, L.M., Vilela, C.L.S., Rosado, J.G., Cardoso, P.M., et al. (2021). Coral microbiome manipulation elicits metabolic and genetic restructuring to mitigate heat stress and evade mortality. Sci. Adv. *7*, eabg3088. https://doi.org/10.1126/sciadv.abg3088.
22. Fragoso Ados Santos, H., Duarte, G.A.S., Rachid, C.T.D.C., Chaloub, R.M., Calderon, E.N., Marangoni, L.F.D.B., Bianchini, A., Nudi, A.H., Do Carmo, F.L., Van Elsas, J.D., et al. (2015). Impact of oil spills on coral reefs can be reduced by bioremediation using probiotic microbiota. Sci. Rep. *5*, 18268. https://doi.org/10.1038/srep18268.
23. Rosado, P.M., Leite, D.C.A., Duarte, G.A.S., Chaloub, R.M., Jospin, G., Nunes Da Rocha, U., Saraiva, J.P., Dini-Andreote, F., Eisen, J.A., Bourne, D.G., et al. (2019). Marine probiotics: increasing coral resistance to bleaching through microbiome manipulation. ISME J. *13*, 921–936. https://doi.org/10.1038/s41396-018-0323-6.
24. Peixoto, R.S., Sweet, M., and Bourne, D.G. (2019). Customized Medicine for Corals. Front. Mar. Sci. *6*, 686. https://doi.org/10.3389/fmars.2019.00686.
25. Doering, T., Wall, M., Putchim, L., Rattanawongwan, T., Schroeder, R., Hentschel, U., and Roik, A. (2021). Towards enhancing coral heat tolerance: a "microbiome transplantation" treatment using inoculations of homogenized coral tissues. Microbiome *9*, 102. https://doi.org/10.1186/s40168-021-01053-6.
26. Dungan, A.M., Hartman, L.M., Blackall, L.L., and Van Oppen, M.J.H. (2022). Exploring microbiome engineering as a strategy for improved thermal tolerance in *Exaiptasia diaphana*. J. Appl. Microbiol. *132*, 2940–2956. https://doi.org/10.1111/jam.15465.
27. Silva, D.P., Villela, H.D.M., Santos, H.F., Duarte, G.A.S., Ribeiro, J.R., Ghizelini, A.M., Vilela, C.L.S., Rosado, P.M., Fazolato, C.S., Santoro, E.P., et al. (2021). Multi-domain probiotic consortium as an alternative to chemical remediation of oil spills at coral reefs and adjacent sites. Microbiome *9*, 118. https://doi.org/10.1186/s40168-021-01041-w.
28. Zhang, Y., Yang, Q., Ling, J., Long, L., Huang, H., Yin, J., Wu, M., Tang, X., Lin, X., Zhang, Y., and Dong, J. (2021). Shifting the microbiome of a coral holobiont and improving host physiology by inoculation with a potentially beneficial bacterial consortium. BMC Microbiol. *21*, 130. https://doi.org/10.1186/s12866-021-02167-5.
29. Ushijima, B., Gunasekera, S.P., Meyer, J.L., Tittl, J., Pitts, K.A., Thompson, S., Sneed, J.M., Ding, Y., Chen, M., Jay Houk, L., et al. (2023). Chemical and genomic characterization of a potential probiotic treatment for stony coral tissue loss disease. Commun. Biol. *6*, 248. https://doi.org/10.1038/s42003-023-04590-y.
30. Li, J., Yang, Q., Dong, J., Sweet, M., Zhang, Y., Liu, C., Zhang, Y., Tang, X., Zhang, W., and Zhang, S. (2023). Microbiome Engineering: A Promising Approach to Improve Coral Health. Engineering *28*, 105–116. https://doi.org/10.1016/j.eng.2022.07.010.
31. Lawson, C.A., Raina, J.B., Kahlke, T., Seymour, J.R., and Suggett, D.J. (2018). Defining the core microbiome of the symbiotic dinoflagellate, *Symbiodinium*. Environ. Microbiol. Rep. *10*, 7–11. https://doi.org/10.1111/1758-2229.12599.
32. Maire, J., Girvan, S.K., Barkla, S.E., Perez-Gonzalez, A., Suggett, D.J., Blackall, L.L., and Van Oppen, M.J.H. (2021). Intracellular bacteria are common and taxonomically diverse in cultured and in hospite algal endosymbionts of coral reefs. ISME J. *15*, 2028–2042. https://doi.org/10.1038/s41396-021-00902-4.
33. Quigley, K.M., Alvarez Roa, C., Torda, G., Bourne, D.G., and Willis, B.L. (2020). Co-dynamics of Symbiodiniaceae and bacterial populations during the first year of symbiosis with *Acropora tenuis* juveniles. MicrobiologyOpen *9*, e959. https://doi.org/10.1002/mbo3.959.
34. Kazandjian, A., Shepherd, V.A., Rodriguez-Lanetty, M., Nordemeier, W., Larkum, A.W.D., and Quinnell, R.G. (2008). Isolation of Symbiosomes and The Symbiosome Membrane Complex from The Zoanthid Zoanthus Robustus. Phycologia *47*, 294–306. https://doi.org/10.2216/PH07-23.1.
35. Peng, S.-E., Wang, Y.-B., Wang, L.-H., Chen, W.-N.U., Lu, C.-Y., Fang, L.-S., and Chen, C.-S. (2010). Proteomic analysis of symbiosome membranes in Cnidaria-dinoflagellate endosymbiosis. Proteomics *10*, 1002–1016. https://doi.org/10.1002/pmic.200900595.
36. Gardner, S.G., Leggat, W., and Ainsworth, T.D. (2023). The microbiome of the endosymbiotic Symbiodiniaceae in corals exposed to thermal stress. Hydrobiologia *850*, 3685–3704. https://doi.org/10.1007/s10750-023-05221-7.
37. Dunkley, P.R., Jarvie, P.E., and Robinson, P.J. (2008). A rapid Percoll gradient procedure for preparation of synaptosomes. Nat. Protoc. *3*, 1718–1728. https://doi.org/10.1038/nprot.2008.171.
38. Garrido, A.G., Machado, L.F., Zilberberg, C., and Leite, D.C.D.A. (2021). Insights into 'Symbiodiniaceae phycosphere' in a coral holobiont. Symbiosis *83*, 25–39. https://doi.org/10.1007/s13199-020-00735-3.
39. Ben-Haim, Y., and Rosenberg, E. (2002). A novel Vibrio sp. pathogen of the coral Pocillopora damicornis. Marine Bio. *141*, 47–55. https://doi.org/10.1007/s00227-002-0797-6.
40. Jacquemot, L., Bettarel, Y., Monjol, J., Corre, E., Halary, S., Desnues, C., Bouvier, T., Ferrier-Pagès, C., and Baudoux, A.-C. (2018). Therapeutic Potential of a New Jumbo Phage That Infects Vibrio coralliilyticus, a Widespread Coral Pathogen. Front. Microbiol. *9*, 2501. https://doi.org/10.3389/fmicb.2018.02501.
41. Sweet, M., Villela, H., Keller-Costa, T., Costa, R., Romano, S., Bourne, D.G., Cárdenas, A., Huggett, M.J., Kerwin, A.H., Kuek, F., et al.

(2021). Insights into the Cultured Bacterial Fraction of Corals. mSystems *6*, e0124920. https://doi.org/10.1128/mSystems.01249-20.
42. Radjasa, O.K., Martens, T., Grossart, H.-P., Sabdono, A., Simon, M., and Bachtiar, T. (2005). Antibacterial Property of a Coral-Associated Bacterium Pseudoalteromonas luteoviolacea Against Shrimp Pathogenic Vibrio harveyi (In Vitro Study). HAYATI J. Biosci. *12*, 77–81. https://doi.org/10.1016/S1978-3019(16)30329-1.
43. Jayasree, V.S., Sobhana, K.S., Priyanka, P., Keerthi, K.R., Jasmine, S., Ranjith, L., Ramkumar, S., Saravanan, R., Kingsley, H.J., Sreenath, K.R., et al. (2021). Characterization and antibacterial activity of violacein producing deep purple pigmented bacterium Pseudoalteromonas luteoviolacea (Gauthier, 1982) isolated from coral reef ecosystems. IJMS *50*, 620–634. https://doi.org/10.56042/ijms.v50i08.40727.
44. Kim, Y.-S., Noh, E.S., Lee, D.-E., and Kim, K.-H. (2017). Complete genome of a denitrifying Halioglobus sp. RR3-57 isolated from a seawater recirculating aquaculture system. Korean J. Microbiol. *53*, 58–60. https://doi.org/10.7845/KJM.2017.7003.
45. Pernice, M., Meibom, A., Van Den Heuvel, A., Kopp, C., Domart-Coulon, I., Hoegh-Guldberg, O., and Dove, S. (2012). A single-cell view of ammonium assimilation in coral–dinoflagellate symbiosis. ISME J. *6*, 1314–1324. https://doi.org/10.1038/ismej.2011.196.
46. Wiedenmann, J., D'Angelo, C., Smith, E.G., Hunt, A.N., Legiret, F.-E., Postle, A.D., and Achterberg, E.P. (2013). Nutrient enrichment can increase the susceptibility of reef corals to bleaching. Nat. Clim. Chang. *3*, 160–164. https://doi.org/10.1038/nclimate1661.
47. Rädecker, N., Pogoreutz, C., Voolstra, C.R., Wiedenmann, J., and Wild, C. (2015). Nitrogen cycling in corals: the key to understanding holobiont functioning? Trends Microbiol. *23*, 490–497. https://doi.org/10.1016/j.tim.2015.03.008.
48. Pereira, L.B., Palermo, B.R.Z., Carlos, C., and Ottoboni, L.M.M. (2017). Diversity and antimicrobial activity of bacteria isolated from different Brazilian coral species. FEMS Microbiol. Lett. *364, fnx164*. https://doi.org/10.1093/femsle/fnx164.
49. Damjanovic, K., Menéndez, P., Blackall, L.L., and van Oppen, M.J.H. (2020). Mixed-mode bacterial transmission in the common brooding coral *Pocillopora acuta*. Environ. Microbiol. *22*, 397–412. https://doi.org/10.1111/1462-2920.14856.
50. Hara, A., Syutsubo, K., and Harayama, S. (2003). Alcanivorax which prevails in oil-contaminated seawater exhibits broad substrate specificity for alkane degradation. Environ. Microbiol. *5*, 746–753. https://doi.org/10.1046/j.1468-2920.2003.00468.x.
51. Silveira, C.B., and Thompson, F. (2014). The Family Alcanivoraceae. In The Prokaryotes, E. Rosenberg, E.F. DeLong, S. Lory, E. Stackebrandt, and F. Thompson, eds. (Springer Berlin Heidelberg), pp. 59–67. https://doi.org/10.1007/978-3-642-38922-1_369.
52. Chernikova, T.N., Bargiela, R., Toshchakov, S.V., Shivaraman, V., Lunev, E.A., Yakimov, M.M., Thomas, D.N., and Golyshin, P.N. (2020). Hydrocarbon-Degrading Bacteria Alcanivorax and Marinobacter Associated With Microalgae Pavlova lutheri and Nannochloropsis oculata. Front. Microbiol. *11*, 572931. https://doi.org/10.3389/fmicb.2020.572931.
53. Rosado, P.M., Cardoso, P.M., Rosado, J.G., Schultz, J., Nunes Da Rocha, U., Keller-Costa, T., and Peixoto, R.S. (2023). Exploring the Potential Molecular Mechanisms of Interactions between a Probiotic Consortium and Its Coral Host. mSystems *8*, e00921-22. https://doi.org/10.1128/msystems.00921-22.
54. Berendsen, R.L., Pieterse, C.M.J., and Bakker, P.A.H.M. (2012). The rhizosphere microbiome and plant health. Trends Plant Sci. *17*, 478–486. https://doi.org/10.1016/j.tplants.2012.04.001.
55. Slightom, R.N., and Buchan, A. (2009). Surface Colonization by Marine Roseobacters: Integrating Genotype and Phenotype. Appl. Environ. Microbiol. *75*, 6027–6037. https://doi.org/10.1128/AEM.01508-09.
56. Seymour, J., Ahmed, T., Durham, W., and Stocker, R. (2010). Chemotactic response of marine bacteria to the extracellular products of Synechococcus and Prochlorococcus. Aquat. Microb. Ecol. *59*, 161–168. https://doi.org/10.3354/ame01400.
57. Camp, E.F., Suggett, D.J., Pogoreutz, C., Nitschke, M.R., Houlbreque, F., Hume, B.C.C., Gardner, S.G., Zampighi, M., Rodolfo-Metalpa, R., and Voolstra, C.R. (2020). Corals exhibit distinct patterns of microbial reorganisation to thrive in an extreme inshore environment. Coral Reefs *39*, 701–716. https://doi.org/10.1007/s00338-019-01889-3.
58. Schatz, D., and Vardi, A. (2018). Extracellular vesicles — new players in cell–cell communication in aquatic environments. Curr. Opin. Microbiol. *43*, 148–154. https://doi.org/10.1016/j.mib.2018.01.014.
59. Marcilla, A., Martin-Jaular, L., Trelis, M., De Menezes-Neto, A., Osuna, A., Bernal, D., Fernandez-Becerra, C., Almeida, I.C., and Del Portillo, H.A. (2014). Extracellular vesicles in parasitic diseases. J. Extracell. Vesicles *3*, 25040. https://doi.org/10.3402/jev.v3.25040.
60. Berg, G., Opelt, K., Zachow, C., Lottmann, J., Götz, M., Costa, R., and Smalla, K. (2006). The rhizosphere effect on bacteria antagonistic towards the pathogenic fungus Verticillium differs depending on plant species and site. FEMS Microbiol. Ecol. *56*, 250–261. https://doi.org/10.1111/j.1574-6941.2005.00025.x.
61. Do Carmo, F.L., Dos Santos, H.F., Martins, E.F., van Elsas, J.D., Rosado, A.S., and Peixoto, R.S. (2011). Bacterial structure and characterization of plant growth promoting and oil degrading bacteria from the rhizospheres of mangrove plants. J. Microbiol. *49*, 535–543. https://doi.org/10.1007/s12275-011-0528-0.
62. Apprill, A., McNally, S., Parsons, R., and Weber, L. (2015). Minor revision to V4 region SSU rRNA 806R gene primer greatly increases detection of SAR11 bacterioplankton. Aquat. Microb. Ecol. *75*, 129–137. https://doi.org/10.3354/ame01753.
63. Parada, A.E., Needham, D.M., and Fuhrman, J.A. (2016). Every base matters: assessing small subunit rRNA primers for marine microbiomes with mock communities, time series and global field samples: Primers for marine microbiome studies. Environ. Microbiol. *18*, 1403–1414. https://doi.org/10.1111/1462-2920.13023.
64. Weisburg, W.G., Barns, S.M., Pelletier, D.A., and Lane, D.J. (1991). 16S ribosomal DNA amplification for phylogenetic study. J. Bacteriol. *173*, 697–703.
65. Hume, B.C.C., Ziegler, M., Poulain, J., Pochon, X., Romac, S., Boissin, E., De Vargas, C., Planes, S., Wincker, P., and Voolstra, C.R. (2018). An improved primer set and amplification protocol with increased specificity and sensitivity targeting the *Symbiodinium* ITS2 region. PeerJ *6*, e4816. https://doi.org/10.7717/peerj.4816.
66. Edgar, R.C. (2016). UNOISE2: improved error-correction for Illumina 16S and ITS amplicon sequencing. Preprint at bioRxiv. https://doi.org/10.1101/081257.
67. Veron, J.E.N. (2000). Corals of the World (Mary Stafford-Smith).
68. Mayfield, A.B., Fan, T.-Y., and Chen, C.-S. (2013). Real-time PCR-Based Gene Expression Analysis in the Model Reef-Building Coral Pocillopora Damicornis: Insight from a Salinity Stress Study. Platax *10*, 1–29.
69. Voolstra, C.R., Quigley, K.M., Davies, S.W., Parkinson, J.E., Peixoto, R.S., Aranda, M., Baker, A.C., Barno, A.R., Barshis, D.J., Benzoni, F., et al. (2021). Consensus Guidelines for Advancing Coral Holobiont Genome and Specimen Voucher Deposition. Front. Mar. Sci. *8*, 701784. https://doi.org/10.3389/fmars.2021.701784.
70. Silva Lima, A.W., Leomil, L., Oliveira, L., Varasteh, T., Thompson, J.R., Medina, M., Thompson, C.C., and Thompson, F.L. (2020). Insights on the genetic repertoire of the coral Mussismilia braziliensis endosymbiont Symbiodinium. Symbiosis *80*, 183–193. https://doi.org/10.1007/s13199-020-00664-1.
71. Hill, L.J., Paradas, W.C., Willemes, M.J., Pereira, M.G., Salomon, P.S., Mariath, R., Moura, R.L., Atella, G.C., Farina, M., Amado-Filho, G.M., and Salgado, L.T. (2019). Acidification-induced cellular changes in Symbiodinium isolated from Mussismilia braziliensis. PLoS One *14*, e0220130. https://doi.org/10.1371/journal.pone.0220130.
72. Cole, J.R., Wang, Q., Cardenas, E., Fish, J., Chai, B., Farris, R.J., Kulam-Syed-Mohideen, A.S., McGarrell, D.M., Marsh, T., Garrity, G.M., and Tiedje, J.M. (2009). The Ribosomal Database Project: improved alignments and new tools for rRNA analysis. Nucleic Acids Res. *37*, D141–D145. https://doi.org/10.1093/nar/gkn879.
73. Hall, T.; Ibis Biosciences, and Carlsbad, C. (2011). BioEdit: An important software for molecular biology. GERF Bull. Biosci. *2*, 60–61.
74. Johnson, M., Zaretskaya, I., Raytselis, Y., Merezhuk, Y., McGinnis, S., and Madden, T.L. (2008). NCBI BLAST: a better web interface. Nucleic Acids Res. *36*, W5–W9. https://doi.org/10.1093/nar/gkn201.
75. Bolger, A.M., Lohse, M., and Usadel, B. (2014). Trimmomatic: a flexible trimmer for Illumina sequence data. Bioinformatics *30*, 2114–2120. https://doi.org/10.1093/bioinformatics/btu170.
76. Wemheuer, B., and Wemheuer, F. (2017). Assessing Bacterial and Fungal Diversity in the Plant Endosphere. In Metagenomics Methods

in Molecular Biology, W.R. Streit and R. Daniel, eds. (Springer), pp. 75–84. https://doi.org/10.1007/978-1-4939-6691-2_6.

77. Love, M.I., Huber, W., and Anders, S. (2014). Moderated estimation of fold change and dispersion for RNA-seq data with DESeq2. Genome Biol. *15*, 550. https://doi.org/10.1186/s13059-014-0550-8.

78. Parks, D.H., Chuvochina, M., Chaumeil, P.-A., Rinke, C., Mussig, A.J., and Hugenholtz, P. (2020). A complete domain-to-species taxonomy for Bacteria and Archaea. Nat. Biotechnol. *38*, 1079–1086. https://doi.org/10.1038/s41587-020-0501-8.

79. Schneider, C.A., Rasband, W.S., and Eliceiri, K.W. (2012). NIH Image to ImageJ: 25 years of image analysis. Nat. Methods *9*, 671–675. https://doi.org/10.1038/nmeth.2089.

80. Oksanen, J., Simpson, G.L., Blanchet, F.G., Kindt, R., Legendre, P., Minchin, P.R., O'Hara, R.B., Solymos, P., Stevens, M.H.H., Szoecs, E., et al. (2022). vegan: Community Ecology Package. R package version 2, 6. https://CRAN.R-project.org/package=vegan.

STAR★METHODS

KEY RESOURCES TABLE

REAGENT or RESOURCE	SOURCE	IDENTIFIER
Biological samples		
Pocillopora damicornis	Ocyan Reef coral farm (Itú, São Paulo, Brazil)	N/A
Chemicals, peptides, and recombinant proteins		
Marine Agar 2216	BD DIFCO™	Cat#212185
Marine Broth 2216	BD DIFCO™	Cat#279110
Percoll®	Cytiva	Cat#GE17-0891-02
DiI stain	ThermoFisher	Cat# D3911
Fluoroshield™ with DAPI	Sigma-Aldrich	Cat# F6057
Critical commercial assays		
Allprep Kit	QIAGEN	Cat# 80204
Genomic DNA Purification Kit	Wizard®	Cat#A1120
Qubit® 2.0 Fluorometer High Sensitivity DNA kit	Thermo Fisher	Cat#Q32851
Deposited data		
Raw amplicon sequencing data	This study/NCBI's SRA	PRJNA936169
Bioinformatic pipeline	This study	https://github.com/LilianHill/in-hospite-Symbiodiniaceae-phycosphere
Oligonucleotides		
EUB-338 conjugated with Alexa Fluor 532	Thermo Fisher	5′- GCTGCCTCCCGTAGGAGT-3′
Non-EUB-338 conjugated with Alexa Fluor 647	Thermo Fisher	5′- ACTCCTACGGGAGGCAGC-3′
515F	Apprill et al.[62]; Parada et al.[63]	5′-GTGYCAGCMGCCGCGGTAA-3′
806R	Apprill et al.[62]; Parada et al.[63]	5′-GGACTACNVGGGTWTCTAAT-3′
27F	Weisburg et al.[64]	5′-AGAGTTTGATCCTGGCTCAG -3′
1492R	Weisburg et al.[64]	5′-CTACGGCTACCTTGTTACGA -3′
SYM_VAR_5.8S2	Hume et al.[65]	5′- GAATTGCAGAACTCCGTGAACC -3′
SYM_VAR_REV	Hume et al.[65]	5′- CGGGTTCWCTTGTYTGACTTCATGC -3′
Software and algorithms		
UCHIME2	Edgar[66]	https://doi.org/10.1101/081257
DESeq2	Love et al.[3]	https://doi.org/10.18129/B9.bioc.DESeq2
Vegan (v.2.6–4)	https://rdrr.io/cran/vegan/	https://github.com/vegandevs/vegan
ggplot2 (v.3.4.0)	https://cran.r-project.org/web/packages/ggplot2/index.html	https://github.com/tidyverse/ggplot2
BioEdit 7.2	Hall [82]	https://bioedit.software.informer.com/7.2/
Other		
syringe needle (21 G × 1″- 0.80 mm × 25 mm)	N/A	N/A
syringe needle (26 G × ½ - 0.45 mm × 13 mm)	N/A	N/A
40 µm nylon cell separator	Falcon®	Cat#352340

RESOURCE AVAILABILITY

Lead contact

Further information and requests for resources and reagents should be directed to and will be fulfilled by the lead contact, Raquel Peixoto (raquel.peixoto@kaust.edu.sa).

Materials availability

- Bacterial strains isolated in this study, and identified in Table S7, have been conserved at the Molecular Microbial Ecology Lab's biobank at the Federal University of Rio de Janeiro - Rio de Janeiro, Brazil.
- The skeletons of the coral fragments used were stored in 70% ethanol and deposited at the Celenterology Collection of the National Museum of the Federal University of Rio Janeiro as vouchers and are detailed in Table S8.
- Materials reported in this paper may be provided by Lilian Hill (lilianhill@ufrj.br) or Raquel Peixoto upon request.

Data and code availability

- Raw amplicon sequencing data are available on NCBI's Read Archive under BioProject ID PRJNA936169. All datasets are publicly available as of the date of publication.
- The complete bioinformatic pipeline including scripts for figure reproduction is publicly available through the GitHub repository at <https://github.com/LilianHill/in-hospite-Symbiodiniaceae-phycosphere>.
- Any additional information required to reanalyze the data reported in this paper is available from the lead contact upon request.

EXPERIMENTAL MODEL AND STUDY PARTICIPANT DETAILS

All experiments in this study were performed with *ex situ* adult fragments of the coral model *Pocillopora damicornis* and/or with *in vitro Symbiodinium* sp. cells (CCMR0100 strain donated by Prof. Paulo Salomon from the Biology Institute of the Federal University of Rio de Janeiro).

METHOD DETAILS

Cellular fractionation and in hospite symbiodiniaceae purification

The purification protocol of *ih*SC and their associated bacteria from the coral model *P. damicornis*[67,68] was adapted from two reference methods, one developed by Peng et al. (2010)[35] to assess the protein content of the symbiosome in the sea anemone *Aiptasia pulchella*, and the other designed to isolate the symbiosome of a zoanthid to characterize the molecular components of its membrane.[34] Our protocol uses different centrifugation regimes and includes microscopy to evaluate the separation and integrity of Symbiodiniaceae cells. Several filtration steps are included to separate bigger and more dense cells (as well as the thick mucus) from the rest of the homogenized. For the development of this protocol, a total of 35 *P damicornis* fragments (i.e., one sample composed of seven fragments, for the obtention of enough biomass, was used for each experiment, which was repeated five times - n = 5) were subjected to the process, as illustrated in Figure 1 and described in detail in the following: Coral tissue was separated from the coral fragments using an airbrush (maximum pressure of 393 kPa) and 15 mL of filtered-sterile artificial seawater (FASW - NaCl 420 mM, $MgSO_4$ 26 mM, $MgCl_2.6H_2O$ 23 mM, KCl 9 mM, $CaCl_2.6H_2O$ 9 mM, $NaHCO_3$ 2 mM, HEPES 10 mM, pH 8.2). An aliquot of raw tissue was kept for further analysis. The remaining raw tissue was passed through a syringe needle (21 G × 1″- 0.80 mm × 25 mm) five times, creating a homogenate that was centrifuged at 100 × g for 1 min to remove cell debris. The supernatant was centrifuged at 200 × g for 28 min, and the pellet was collected, resuspended in FASW, and passed through a syringe needle (26 G × ½ - 0.45 mm × 13 mm) five times. This homogenate was syringe-filtered through a sterile 40 μm nylon cell separator (Falcon #352340) to disrupt lumps. The filtrate was then purified by centrifugation in a discontinuous gradient of solution of isotonic Percoll (SIP) of four different concentrations (i.e., 25%, 50%, 80%, and 100% - details bellow) and centrifuged at 800 × g for 20 min. The contents corresponding to each fraction of the gradient plus the upper layer above the 25% SIP fraction (i.e., 0% SIP fraction) (Figure S1) were collected in separate tubes and centrifuged at 200 × g for 20 min. The Percoll was removed by washing the pellet three times in FASW. The pellets were then resuspended in 2mL of FASW and stored for further analysis (i.e., fixed for microscopy or frozen at −80°C for molecular analysis). All centrifugations were made with a fixed rotor centrifuge at room temperature (~25°C).

The solution of isotonic Percoll (SIP) was prepared by mixing 9 parts (v/v) Percoll (Cytiva #GE17-0891-02) with 1 part (v/v) 1.5 M NaCl, according to the manufacturer's instructions. To create the discontinuous gradient, 15 mL of SIP (13.5 mL of Percoll and 1.5 mL of 1.5 M NaCl) was used as 100% SIP. The gradient was then created by adding different amounts of SIP to aliquots of filtered artificial seawater (FASW), resulting in gradients of 80%, 50%, and 25% SIP. The gradient was assembled in a sterile 15 mL falcon centrifuge tube containing 2 mL of 100% SIP, 2 mL of 80% SIP, 5 mL of 50% SIP, and 4 mL of 25% SIP (Figure S1).

All fragments were photographed on a Coral Health Chart before and after tissue removal to record their size and health conditions. The remaining skeletons were stored in 70% ethanol and deposited at the Celenterology Collection of the National Museum of the Federal University of Rio Janeiro (MN/UFRJ) as recommended by Voolstra et al. (2021)[69] – details about vouchers are in Table S8.

Cellular integrity assessment of symbiodiniaceae fraction

The final products (i.e., the SIP fractions and the raw samples) obtained from the separation of *ih*SC from the *P. damicornis* fragments were used to count and evaluate cell individualization using a Neubauer chamber and integrity using fluorescence staining. For the latter, 100 μL of each fraction were stained with 20 mM DiI dye (ThermoFisher, Waltham, MA, USA) for 1 h in the dark. DiI staining was performed for a first assessment of the integrity of Symbiodiniaceae lipid membranes (and therefore the cellular integrity), after the fractionation procedure. A more refined TEM analysis was then performed to also assess the presence, ultrastructure and integrity of recovered symbiosomes. After incubation, samples were washed twice with 100 μL FASW and centrifuged at 100 × g for 7 min. Samples were visualized with an Axio Imager D2

(Zeiss, Jena, Germany) in bright field and using the 546/12 nm–590 nm filter for chlorophyll autofluorescence and the 450/490 nm–515/565 nm filter to detect lipid membranes stained by DiI. Pure cultures of Symbiodiniaceae (CCMR0100 strain isolated from *Mussismilia braziliensis*, corresponding to *Symbiodinium* sp. clade A4)[70] were used as a positive control.

Based on the cell counting results, the 50% SIP fraction and samples of raw tissue were processed to visualize the ultrastructure of Symbiodiniaceae cells and analyze the cellular integrity (including symbiosome membranes) using TEM. Processing was performed as described by Hill et al. (2019).[71] Briefly, 250 μL of each sample was added to 250 μL of a fixative solution composed of 2% glutaraldehyde, 0.1M sodium cacodylate buffer, and 0.3M of sucrose. Samples were fixed for 1 h and rinsed in 0.1M sodium cacodylate buffers with decreasing concentrations of sucrose (i.e., 0.3M, 0.15M, 0.075M, and 0). These samples were then post-fixed in 1% osmium tetraoxide for 1 h and washed three times with 0.1M sodium cacodylate buffer. Dehydration was then performed in an acetone series (30%, 40%, 50%, 70%, 80%, 90%, and 3 × 100%), and samples were embedded in Spurr resin. Ultrathin sections (~70 nm) were obtained on a Leica EM UC6 ultramicrotome with a diamond knife (Diatome, Hatfield, PA, USA) and collected on 300 mesh copper grids. After staining in uranyl acetate and lead citrate, sections were examined with a Hitachi HT7800 electron microscope.

Analysis of *in hospite* symbiodiniaceae-associated bacteria

Samples of each fraction and the raw tissue were plated for bacterial isolation and colony forming unit (CFU) counts, processed for fluorescence *in situ* hybridization (FISH) to localize bacteria cells attached to Symbiodiniaceae cells, and processed for 16S rRNA gene and ITS2 region sequencing.

Bacterial isolation and taxonomic identification of isolates

For bacterial isolation, serial dilutions of final samples obtained from each SIP fraction from each replicate (n = 5) were plated in triplicate onto Marine Agar (Marine Agar Zobell 2216, Himedia Laboratories, Mumbai, India). A plate without inoculum and another plate containing the Percoll solution without sample were used as negative controls. CFUs were counted 18 h after incubation at 28°C on the plates with counts between 30 and 300 CFUs. A total of 38 bacterial colonies representing different morphologies were selected from all fractions in all replicates for subsequent streak plate isolation on Marine Agar. The pure colonies were incubated in 5 mL of Marine Broth (MB) for 18 h at 28°C with constant agitation at 120 rpm. After incubation and growth, 800 μL of the cultures were transferred to cryotubes containing 200 μL of 80% glycerol and stored at −80°C. The purity of bacterial growth used for the stock was confirmed with a new inoculum on a streak plate in MA incubated for 18 h at 28°C.

Total genomic DNA was extracted from bacterial isolates for taxonomic identification based on 16S rRNA gene sequencing. DNA extraction was performed using the Wizard Genomic DNA Purification Kit (Promega, United States of America). The quality and concentration of the extracted nucleic acids were assessed using a NanoDrop 1000 (Thermo Fisher Scientific, Waltham, MA, USA) and a Qubit 2.0 Fluorometer High Sensitivity DNA kit (Thermo Fisher Scientific, Waltham, MA, USA), respectively. The bacterial 16S rRNA gene was amplified using the primers 27F (5′-AGA GTT TGA TCA TGG CTC AG-3′) and 1492R (5′-GTT TAC CTT GTT ACG ACT T-3′).[64] Amplification was verified by 1.2% agarose gel electrophoresis. The PCR products were sequenced on an AB3730XL sequencer (Thermo Fischer Scientific, Waltham, MA, USA) at the Ramaciotti Center for Genomics (University of New South Wales, Sydney, Australia). Raw reads were deposited in NCBI within BioProject ID PRJNA936169.

16S rRNA gene sequences were processed through the Ribosomal Database Project (RDP),[72] which eliminated low-quality sequences with the parameters: base score <20, error probability >0.01, 0.8 fractions> Q20, and length 400. The forward and reverse reads were assembled with the CAP assembler in the BioEdit Sequence Alignment Editor program.[73] The assembled contigs were compared to the NT database at the National Center for Biotechnology Information (NCBI) using the Basic Local Alignment Search Tool for Nucleotides algorithm (BLASTn).[74] The assembled contigs were also submitted to the Seqmatch tool in RDP. Reference sequences from both databases were used to build phylogenetic trees.

Microbial community analysis

DNA was extracted from samples from all fractions and raw coral tissue with the Allprep kit (Qiagen) according to the manufacturer's instructions. To access the prokaryotic profiles (i.e., bacteria and archaea) associated with the different fractions and raw coral tissue, the V4 hypervariable region of the 16S rRNA gene was amplified using the modified primer pairs 515F (Parada)-806R(Apprill).[62,63] The ITS2 region of Symbiodiniaceae was amplified using the primer pairs SYM_VAR_5.8S2 and SYM_VAR_REV with the addition of MiSeq adapter sequences, as described by Hume et al.[65]

The amplicons were sequenced on a Miseq platform at the Ramaciotti Center for Genomics (University of New South Wales, Sydney, Australia). Raw sequences were quality-filtered using Trimmomatic (version 0.38) in a sliding window of 4 bp, and reads with a quality score below 20 or shorter than 100 bp were discarded.[75,76] Paired-end reads were merged using USEARCH (version 11.0.667), and reads shorter than 260 bp or longer than 310 bp were removed. UNOISE algorithm was used to cluster, denoise and generate ASVs. Chimeras were removed using the UCHIME2 algorithm (high confidence mode).[66] Three samples (DF6, DF36, and DF37; 0% SIP fraction, pure Percoll, and negative extraction control, respectively) were removed from the dataset due to a low number of reads (<2,000). Taxaplot from pure Percoll and negative extraction control can be found in Figure S7. Data were normalized for read counts using the DESeq2 package.[77]

Taxonomy was assigned to the bacterial and archaeal ASV sequences using the BLCA algorithm (identity and coverage intervals set to 95%–100%) against the Genome Taxonomy Database (GTDB version 207).[78] All non-bacterial and non-archaeal ASV sequences were

removed, and reads were mapped to the remaining ASV sequences to estimate the relative abundances. The data were visualized using R version 4.0.2. Symbiodiniaceae taxonomy based on the ITS2 gene was assigned using the BLASTn algorithm against the NCBI database.

Bacterial cell visualization

Bacterial cells and aggregates associated with Symbiodiniaceae cells *in hospite* were visualized by FISH. For this, all samples were fixed immediately after collection in 4% paraformaldehyde overnight at 4°C, rinsed in a solution of Phosphate Buffered Saline (PBS): 100% ethanol (EtOH) (1:1, v/v) for 5 min and kept in PBS at 4°C. Then, samples were dehydrated in a EtOH series (30, 50, 70, 90, 3 × 100%) and embedded in LR White resin at 4°C (1:1 EtOH:LR White overnight, 2 × 100% LR White for 1 h each). Samples were polymerized in BEEM capsules at −20°C under UV light for five days. Thin sections (~1 μm) were made and collected on microscopy slides. For hybridization, sections were first treated with a solution composed of 50 μg/mL proteinase K + 20mM Tris HCl buffer to permeabilize cell membranes. Sections were then covered with a hybridization buffer (formamide 30% + 0.9M NaCl +20mM Tris HCl +0.01% SDS), and probes were added to a final concentration of 25 ng/μL. Serial sections were hybridized separately with a general probe for bacteria (Thermo Fisher; EUB-338; GCTGCCTCCCGTAGGAGT) conjugated with Alexa Fluor 532 and a nonsense probe as negative control (Thermo Fisher; Non-EUB-338; ACTCCTACGGGAGGCAGC) conjugated with Alexa Fluor 647. Samples were then incubated in the dark at 46°C for 1.5 h. Subsequently, sections were washed in a buffer (0.112M NaCl +20mM Tris HCl +0.01% SDS + 5mM EDTA) at 48°C for 10 min and rinsed in cold RNAse/DNAse free water to remove remaining salts. Finally, sections were dried and mounted in Fluoroshield + Dapi (Sigma-Aldrich). All samples were observed in a Leica SPE Confocal Laser Scanning Microscope, with an excitation laser set at 532 nm (for the Alexa Fluor 532), 635 nm (for the Alexa Fluor 647) and 405 nm (for DAPI), and emission bands of 540–560 nm (for Alexa Fluor 532), 640–680 nm (for Alexa Fluor 647) and 400–515 nm (for DAPI). Stack images (confocal depths between 3 and 5 μm) were processed using ImageJ[79] to build maximum intensity z stack and 3D reconstruction videos, and specific lookup tables with virtual colors were attributed to each fluorescent channel in order to contribute with visualization.

QUANTIFICATION AND STATISTICAL ANALYSIS

The experiment was conducted with a total of 35 *P damicornis* fragments, as one sample composed of seven coral fragments was used for each experiment, which was repeated five times (n = 5). The means of Symbiodiniaceae's cells and CFU counts for each SIP fraction were compared within each other using Kruskal-Wallis and Dunn's test.

Alpha-diversity indexes (Chao1 and Shannon) were generated and compared (i.e., Kruskal-Wallis test) using R (version 4.1.2, package stats v.3.6.2), using the results from 16S rRNA gene sequencing. Beta-diversity was calculated and visualized through non-metric multidimensional scaling (nMDS) based on both Sorensen's similarity and Bray-Curtis dissimilarity. Finally, differences in microbial community structure throughout the SIP fractions were tested by performing a permutational multivariate analysis of variance (PERMANOVA) with pairwise comparisons. Differences in the dispersions of the SIP fractions were tested with a permutational multivariate analysis of dispersion (PERMDISP) in R (version 4.1.2) with the package Vegan.[80]

Moreover, we used IndicSpecies analysis to characterize ASVs that are "indicators" for groups of samples. We used func = "IndVal.g" and set the number of permutations to 9999. We filtered the data by excluding ASVs with a p value ≤ 0.02, which were then used in a network interactions analysis using the SpiecEasi package implemented in R, with "mb" method and 100 replicates (lambda.min.ratio = 0.02, nlambda = 200). ASVs with Stat value (IndVal.g) < 0.6 were excluded before analysis. Matrices were exported and used to plot in Cytoscape.